Absence of Fermi surface reconstruction in pressure-driven overdoped YBCO

Stanley W. Tozer,[1,*] William A. Coniglio,[1] Tobias Förster,[2] Doug A. Bonn,[3] Walter N. Hardy,[3] Ruixing Liang,[3] Erik Kampert,[2,4] and Audrey D. Grockowiak[1,5,6,†]

[1]*National High Magnetic Field Laboratory (NHMFL), Florida State University, Tallahassee, Florida 32310, USA*
[2]*Hochfeld-Magnetlabor Dresden (HLD-EMFL), Helmholtz-Zentrum Dresden-Rossendorf, 01328 Dresden, Germany*
[3]*Department of Physics and Astronomy, University of British Columbia, Vancouver, British Columbia V6T 1Z4, Canada*
[4]*Institute of Fundamentals of Electrical Engineering, Helmut Schmidt University, 22043 Hamburg, Germany*
[5]*Brazilian Synchrotron Light Laboratory (LNLS/Sirius), Brazilian Center for Research in Energy and Materials (CNPEM), Campinas 13083-100, Brazil*
[6]*Leibniz-Institut für Festkörper- und Werkstoffforschung Dresden, 01069 Dresden, Germany*

(Received 5 December 2023; accepted 16 September 2024; published 9 October 2024)

The evolution of the critical superconducting temperature and field, quantum oscillation frequencies, and effective mass m^* in underdoped $YBa_2Cu_3O_{7-\delta}$ (YBCO) crystals ($p = 0.11$, with p the hole concentration per Cu atom) points to a partial suppression of the charge orders with increasing pressure up to 7 GPa, mimicking doping. Application of pressures up to 25 GPa pushes the sample to the overdoped side of the superconducting dome. In contrast to other cuprates, or to doping studies on YBCO, the frequencies of the quantum oscillations measured in that pressure range do not support the picture of a Fermi-surface reconstruction in the overdoped regime, but possibly point to the existence of a new charge order.

DOI: 10.1103/PhysRevB.110.144508

I. INTRODUCTION

The pnictides, cuprates, and molecular conductors exhibit similar features, hinting at a common mechanism anchored in a universal phase diagram, encompassing antiferromagnetism, superconductivity, and potential quantum critical points (QCPs). Chemical doping is a traditional means to look at such phenomena.

The temperature-oxygen doping phase diagram of $YBa_2Cu_3O_{7-\delta}$ (YBCO) is rich, and exhibits an antiferromagnetic region at the lowest doping. With increasing doping, a superconducting dome develops [1], commencing at $p = 0.05$, extending to an optimal level of $p = 0.16$, up to a maximum doping reached of $p = 0.177$. A distinctive shoulder at $p = 0.08$ is associated with a Fermi surface reconstruction (FSR) [2] as indicated by a change in sign of the Hall [3,4] and Seebeck coefficients [5] (positive to negative at low temperatures), as well as at high magnetic fields. Studies utilizing nuclear magnetic resonance (NMR) [6] and x-ray diffraction (XRD) [7] attribute this to a two-dimensional charge order (CO) peaking around $p = 0.12$. Subsequently, XRD [8], ultrasound [9], and NMR measurements [10] unveiled a field-induced three-dimensional charge order within this doping range, reproduced under zero field via uniaxial strain along the a axis of the orthorhombic structure [11].

Upon oxygen doping, the FS evolves from a small closed electron pocket [12] into a larger, coherent three-dimensional FS on the overdoped side [13,14]. This characterization is derived from examining charge-carrier concentration in copper-oxygen planes of various cuprates, notably $Tl_2Ba_2CuO_{6+\delta}$, the overdoped YBCO analog [15]. The only study showing a FSR, from underdoped to overdoped within one material, was carried out on electron-doped $Nd_{2-x}Ce_xCuO_4$ via Shubnikov–de Haas (SdH) oscillations [16].

The mechanism of the FSR holds pivotal significance in understanding the cuprates and their universal phase diagram. Studying the Fermi surface through quantum oscillations (QOs) requires suppressing superconductivity to examine the material's normal state. Magnetic fields are used to suppress superconductivity, allowing the observation of QOs; however, due to the high superconducting critical transition temperature (T_c) and critical field (H_{c2}), this would require fields in excess of 100 T for samples near optimal doping [17], beyond that currently available in nondestructive magnets. Instead, Zn doping has been used to suppress T_c to about 30 K [18], but doping to these levels introduces impurities and thus scattering, which precludes the observation of QOs.

To date, high pressure studies look mostly at the evolution of T_c with pressure [19–22]. Here, we have used quasihydrostatic pressure to tune the FS of YBCO6.5 starting from the underdoped region, and progressing through the superconducting dome. Measuring the evolution of QOs with pressure and temperature provided direct access to the FSs and effective masses of the charge carriers, which showed a lack of FSR, and possibly points to the existence of a CO similar to the that found on the underdoped side.

II. EXPERIMENTAL METHODS

High purity twinned single crystals of YBCO6.5 ($p = 0.11$, $T_c = 63.3 \pm 1.0$ K) were used to perform SdH

*Contact author: tozer@magnet.fsu.edu
†Contact author: a.grockowiak@ifw-dresden.de

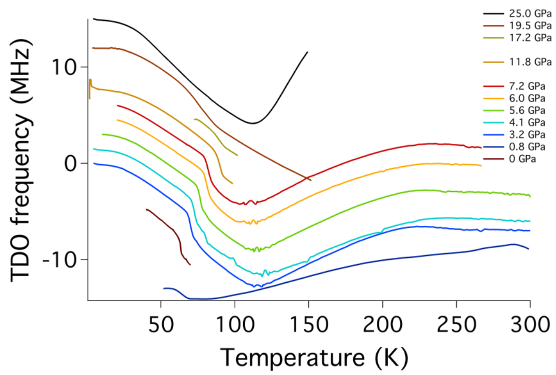

FIG. 1. Evolution of the TDO frequency vs temperature for several pressures at 0 T. The minima observed in the signals at 115 K is an experimental artifact due to crossover of frequency mixing.

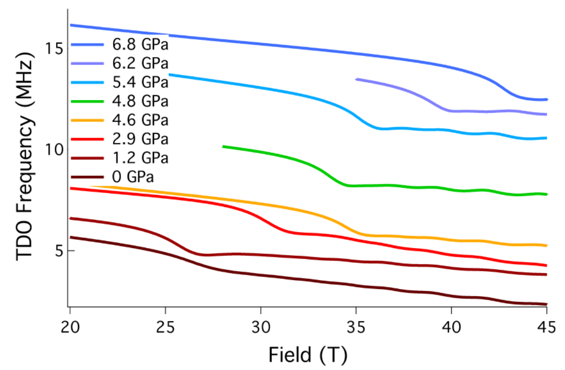

FIG. 2. TDO frequencies vs magnetic field for several pressures at 400 mK (vertically shifted for clarity). QOs are visible above the critical field.

measurements under pressure, between 350 mK and 10 K in DC fields up to 45 T and up to 25 GPa at the NHMFL using metallic diamond anvil cells (DACs), and in pulsed fields up to 80 T and 7 GPa at HDL-EMFL using plastic DACs [23], rotators, and cryogenic tails. The sample was coupled to a resonant LC tank circuit driven by a tunnel diode oscillator (TDO). The coil that makes the inductor of this circuit resided in the sample space of the DAC and sensed changes in resistivity due to variations in temperature, pressure, or magnetic field; see Supplemental Material (SM) [24]. Data were taken with the *c* axis of the crystal oriented parallel to the magnetic field.

III. RESULTS

A. Pressure effect on T_c in zero field

In our study, the pressure was changed at room temperature, and was only increased. The vertical thermal gradient existing in cryostats in DC fields or pulsed magnets makes any accurate determination of T_c difficult. Careful T_c measurements were performed in a 16 T physical property measurement system (PPMS), with the pressure being measured at the transition temperature. Figure 1 shows the evolution of the TDO frequency with temperature for various pressures. We define T_c as the minimum of the derivative of the signal around 80 K for the pressures up to 7.2 GPa (SM Fig. 3 [24]), over which range T_c smoothly increases up 81.2 K. At 19.5 GPa, T_c decreases to 75 K, pointing to the sample having been driven to the overdoped side of the superconducting dome. At 25 GPa, we do not observe a similar kink down to 2 K, and the minimum around 100 K cannot be interpreted as a T_c, as applied fields of 16 T did not shift it to lower temperatures (SM Fig. 4 [24]). Rather, a combination of nonhydrostaticity and pressure variation upon cooling can explain the lack of T_c, both of which tend to broaden transitions which make T_c more difficult to measure. The cells used at higher pressure also have a larger variation in pressure with temperature: we measured an increase in pressure of roughly 20% between room temperature and ^{4}He. For additional details on TDO measurements as a function of temperature, see the Supplemental Material [24].

B. Pressure effect on the critical field

1. Pressures lower than 10 GPa

In Fig. 2, a clear trend in H_{c2} appears, increasing in a nonmonotonic fashion up to 6.8 GPa, where H_{c2} is about 44 T. DC fields limit our study to about 6 GPa on the underdoped side of the superconducting dome of YBCO. Pulsed magnetic fields are required to measure the evolution of H_{c2} and QOs for the higher pressure range. Figure 3 shows an example of data obtained in a 70 T magnet during a 150 ms pulse for a YBCO6.5 sample. The main panel shows the as-measured TDO frequency, where the transition at about 25 T is identified as the superconducting critical field H_{c2}, in agreement with reported resistivity data [17]. Above this transition, clear QOs are observed, and thus we will use this as the marker for H_{c2}. The two traces correspond to the data taken during the up and down sweeps in magnetic field, with overlapping traces indicating that there is no heating of the sample during the pulse. The background-subtracted data above H_{c2} are shown in the top panel, with one frequency clearly observed, confirmed by the fast Fourier transform (FFT) (bottom left). Similar data were obtained up to 7 GPa in an 85 T magnet (SM Fig. 5 [24]).

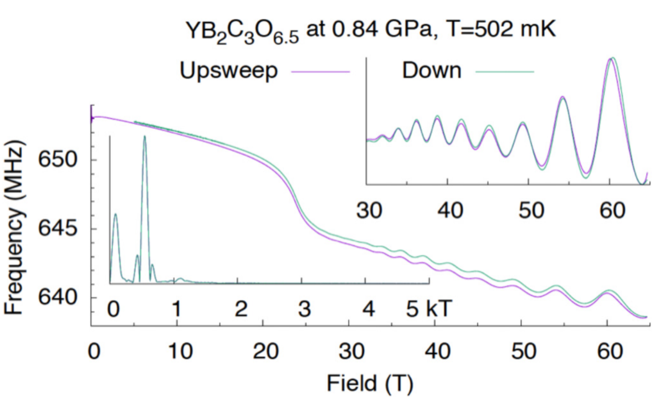

FIG. 3. TDO frequency vs magnetic field. Top panel: oscillatory-part background-subtracted data above H_{c2}. Bottom panel: background-subtracted FFT. The lower frequency peak is a data analysis artifact arising from the polynomial background subtraction.

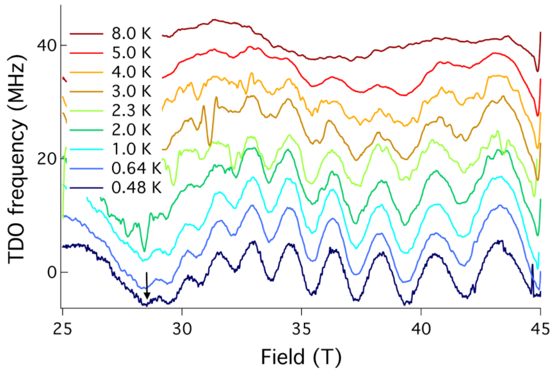

FIG. 4. Evolution of the background-subtracted TDO frequency with field for various temperatures at 18.8 GPa. We assign the minimum in the signal before the onset of the QOs to H_{c2}, indicated by an arrow. The traces are vertically shifted for clarity.

2. Pressures greater than 18 GPa

The estimated values of H_{c2} as one approaches optimal doping are greater than the magnetic fields available in nondestructive pulsed magnets, therefore higher pressures were used to drive the sample to the overdoped side. Three different pressure cells were loaded with a 4:1 methanol:ethanol mixture to 18.8, 20.0, and 25 GPa at low temperatures. Alireza *et al.* [19] used a similar approach and reconstructed the overdoped side of the superconducting dome by applying up to 25 GPa to an optimally doped sample.

Supplemental Material Fig. 6 [24] shows the background-subtracted TDO-frequency field-dependence at base ^{3}He temperatures. The 18.8 GPa cell shows a clear minimum in the signal at 28.4 T (indicated by an arrow) followed by the onset of QOs. Again, we identify this minimum as the critical field. This feature is not as pronounced for higher pressures, but QOs are still observable.

Figure 4 shows the evolution of the background-subtracted TDO frequency with field for various temperatures for YBCO6.5 at 18.8 GPa. The critical field is clearly suppressed with increasing temperature. We plot H_{c2} vs temperature for various pressures in SM Fig. 11 [24], and show that the temperature dependence of the transition at 18.8 GPa follows the same trend.

C. High pressure fermiology

For each pressure, field sweeps were performed at various temperatures to study the temperature dependence of the QO amplitude, as shown in SM Fig. 8(a) for 4.8 GPa and in SM Fig. 7 for 25 GPa [24]. The oscillatory part is plotted as a function of $1/B$, interpolated and smoothed with a Savitzky-Golay filter [25]. A smooth background is subtracted, and the FFT of the result is taken using a Hamming window. The amplitude $A(T)$ of each Fourier transform peak is then plotted versus temperature as shown in SM Fig. 8(b), and fitted using the Lifshitz-Kosevitch (LK) theory (1) for the temperature damping factor [26]:

$$A(T) = A_0 \frac{\alpha m^* T/B}{\sinh(\alpha m^* T/B)}, \tag{1}$$

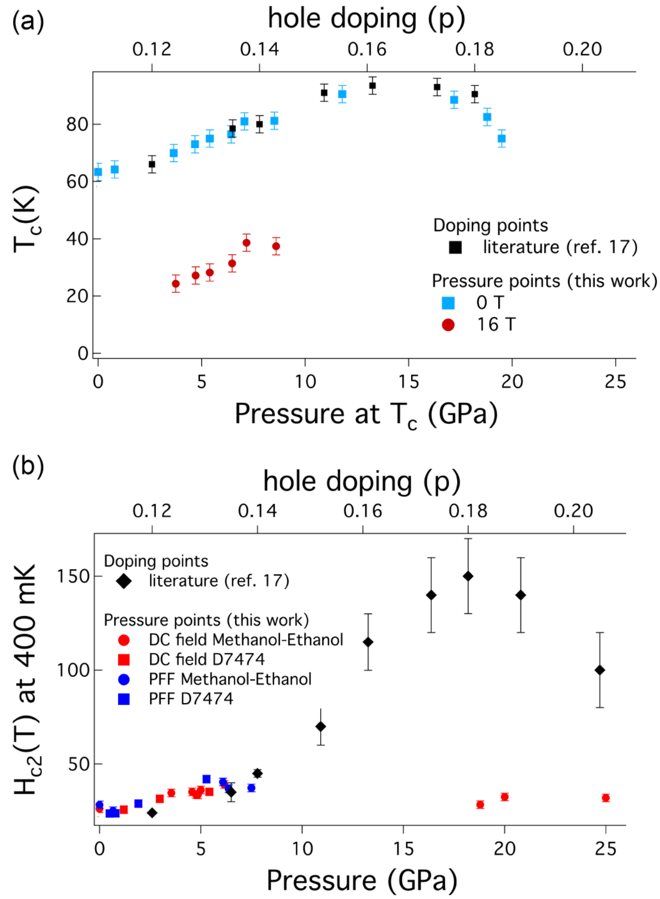

FIG. 5. (a) T_c vs pressure, at 0 and 16 T. The pressure is measured at $T = T_c$. (b) H_{c2} at base ^{3}He temperature as a function of pressure. The data points are separated depending on the pressure medium and magnet used. T_c and H_{c2} vs doping data taken from [17].

where A_0 is a prefactor, $\alpha = 2\pi^2 k_B m_e/e\hbar = 14.69$ T/K, k_B and $\hbar$ the Boltzmann and Planck constants, e the electron charge, and B the harmonic mean of the oscillatory field range. This LK fit gives the effective mass $m^\star$ in units of the free-electron mass m_e of the carrier for that orbit. The observation of QOs requires high-purity crystals with minimal scattering, and hydrostatic conditions. Despite nonhydrostatic conditions for the cells at pressure higher than 15 GPa, clear QOs are observed in SM Fig. 6 [24] with their temperature evolution in SM Fig. 7. The high bulk modulus of YBCO makes it less susceptible to strains due to pressure gradients as suggested by Tateiwa *et al.* [27]. Supplemental Material Fig. 9 shows the oscillatory part of the TDO signal at about 400 mK for various pressures with $1/B$, with the 25 GPa curve multiplied by 10 for better visibility. Comparable SdH frequencies are observed throughout the pressure range.

IV. DISCUSSION

Figure 5(a) shows the evolution of T_c with pressure, increasing from 69.9 K at 3.65 GPa up to 81.2 K at 8.5 GPa. This yields a $dT_c/dP \approx 2.3$ K/GPa, in agreement with previous studies [28–30]. Previous attempts to explain the evolution of the superconducting transition with pressure P [30,31] invoke two main mechanisms described by

$$\frac{dT_c}{dP} = \left(\frac{\partial T_c}{\partial n_h}\right)\left(\frac{\partial n_h}{\partial P}\right) + \left(\frac{dT_c}{dP}\right)_{\text{intrinsic}}, \quad (2)$$

The first term on the right-hand side accounts for an increase of T_c due to an increase in hole doping n_h via a charge transfer between the CuO chains and the CuO plane. The second term encompasses intrinsic effects, such as the increase of oxygen ordering in the CuO chains upon pressure. These intrinsic effects have been extensively studied [28], and showed that the application of pressure at room temperature increases this ordering process, as opposed to applying the pressure at lower temperatures where oxygen chains are frozen. Following the reasoning of Cyr-Choinière *et al.* [29], we compare our dT_c/dP value to those reported by studies in which those effects are minimized, and find a comparable value. In order to estimate the change of doping with pressure, we thus neglect the intrinsic pressure effects on T_c. Previous studies have attempted to quantify this change:

$$n_h(P) = n_{h,0} + \frac{dn_h(P)}{d\epsilon(P)}\epsilon(P), \quad (3)$$

where $n_{h,0}$ is the initial hole doping (also denoted p), and $\epsilon(P)$ is the change in unit-cell volume.

We apply the first-order Murnaghan equation of state [19,32]:

$$\frac{dn_h(P)}{d\epsilon(P)} = n_h'(P)B_0\left(1 + \frac{B_0'}{B_0}P\right)^{1+1/B_0'}, \quad (4)$$

$$\epsilon(p) = 1 - \left(1 + \frac{B_0'}{B_0}p\right)^{-1/B_0'}, \quad (5)$$

where B_0 is the bulk modulus and B_0' its pressure derivative at zero pressure, and $n_h' = dn_h(P)/d(P)$. Comparing our point of $T_c = 81$ K at 7.07 GPa, with reported T_c values with doping [17], we estimate the hole doping at that pressure to be about $n_h(7.07\text{ GPa}) = 0.142$ holes/Cu. Using approximation of values reported from XRD data and calculations for various neighboring dopings of YBCO [33], we use $B_0 \approx 140 \pm 15$ GPa and $B_0' \approx 5.5 \pm 0.1$, which yields $dn_h(P)/d(P)(7.07\text{ GPa}) \approx 0.37 \pm 0.1\%$ hole/GPa, in agreement with recent NMR studies [30].

Figure 5(b) shows the evolution of H_{c2} with pressure, along with a comparison of the evolution in doping (data points from [17] and references therein). The pressure-doping comparison is consistent at pressures below 8 GPa. Our initial decrease in H_{c2} with a minimum at 0.8 GPa matches that observed near $p = 0.12$. The $H_{c2} = 28.4$ T observed for 18.8 GPa places this sample on the overdoped side of the YBCO superconducting dome, making it the first direct measurement of the critical field of overdoped YBCO. The pressure-doping equivalence previously estimated gives $p \approx 0.18$. Our H_{c2} value is, however, in discrepancy with previous measurements reporting $H_{c2} = 150 \pm 20$ T for this doping. Comparing reported H_{c2} values with ours would indicate a doping near $p = 0.24$. The pressure-doping equivalence calculated clearly breaks down at higher pressure, possibly indicating that neglected intrinsic effects should be considered. Those effects can create strains along the different axes of the sample. Several studies have looked into uniaxial compression effects on YBCO. Kim

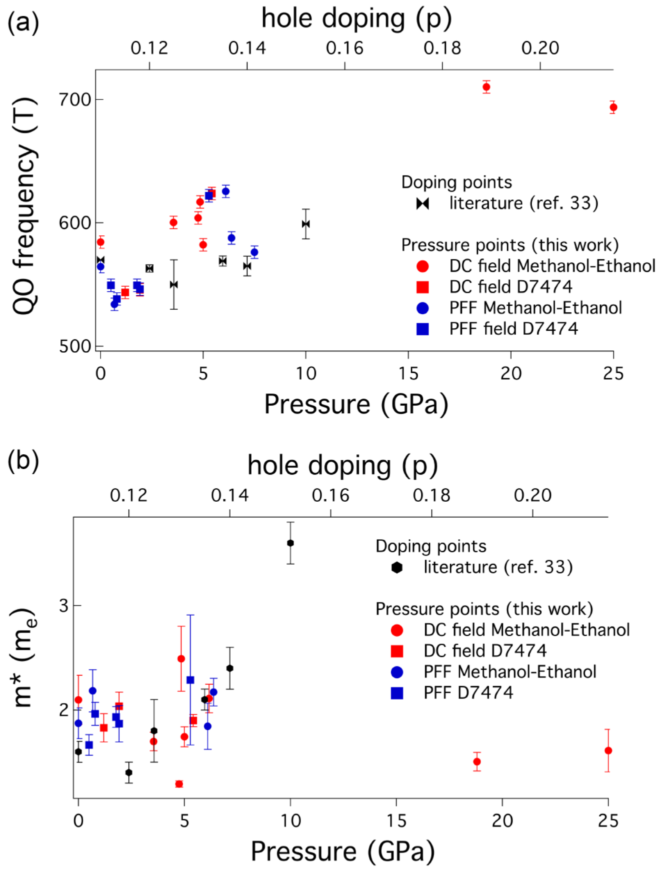

FIG. 6. (a) QO frequencies measured vs pressure. (b) Effective masses m^* vs pressure. The doping data points are taken from [34] and references therein.

et al., in particular [11], have suggested a three-dimensional CO upon compression of the a axis in zero magnetic field. Thus, one option to explain the discrepancy observed in H_{c2} which could be investigated by high pressure NMR, would be the existence of a competing CO created at nonhydrostatic pressures akin to strain.

Figure 6(a) and 6(b) show, respectively, the evolution of the QO frequency and their effective masses with pressure. The data points for comparison with doping are taken from [34] and references within. The QO frequency range observed in our study, 550–650 T, is in excellent agreement with reported data. We observe a minimum in frequency at 0.8 GPa, similar to that observed in H_{c2}, and a possible maximum near 6 GPa. The values are consistent between DC and pulsed-field measurements, and no clear influence of the pressure medium is observed. The $m^\star$ obtained from LK fits are in the range of $1.5m_e$–$2.5m_e$, also in agreement with reported data. We note a minimum in $m^\star$ near 4 GPa. Our low-pressure range does not extend far enough in p to observe the divergence in $m^\star$ noted by Ramshaw *et al.* [34]. For pressures greater than 18 GPa in the overdoped regime, we obtain 710 ± 10 T for 18.8 GPa, and 694 ± 10 T at 25 GPa. The corresponding $m^\star$ are $1.50 \pm 0.08\, m_e$ and $1.6 \pm 0.2\, m_e$, respectively. This is in disagreement with the proposed picture of a FSR for overdoped samples based on measurements of $Tl_2Ba_2CuO_{6+\delta}$, that were shown by angle-dependent magnetoresistance oscillations (AMRO) [13,35] and ARPES measurements [36,37] to have a large coherent three-dimensional Fermi surface. Resistivity and torque measurements at ambient pressure [38] have revealed QOs with a frequency of 18 kT $\pm$ 50 T and an effective mass $m^\star = 4.1 \pm 1.0\, m_e$. The low H_{c2} values at high pressure and negligible change in QO frequency from low to high pressures do not support the picture of a FSR across the superconducting dome, and rather point to the existence of a CO similar to the one observed at low pressure and on the underdoped side.

V. CONCLUSION

Our high pressure TDO measurements of YBCO6.5 have enabled direct measurement of T_c, H_{c2}, and QOs, from which we derived QO frequencies and effective masses. Measurements at pressures below 8 GPa show results in excellent agreement with previous doping studies, confirming the equivalence of pressure and doping. We estimated the value for a charge transfer with pressure and found it to be compatible with other data [30]. The pressure dependencies of H_{c2} and the QO frequency indicates also a suppression of the CO with applied pressure. By applying pressures larger than 18 GPa, the sample was driven to the overdoped regime on the other side of the superconducting dome, as shown by the measured values of T_c and H_{c2}. However, the QO frequencies measured, comparable to those obtained at lower pressure, do not support the picture of a FSR in the overdoped regime of YBCO, but rather indicate the existence of a CO in competition with the superconducting state. High pressure x-ray and NMR measurements should shed light on the origin of this CO and inform on its links to the low pressure, low-doping ones reported.

ACKNOWLEDGMENTS

This work was funded by the DOE/NNSA under DE-NA0001979 and was performed at the National High Magnetic Field Laboratory, which is supported by NSF Cooperative Agreement No. DMR-1157490 and by the State of Florida. Part of this work was supported as part of the Center for Actinide Science and Technology (CAST), an Energy Frontier Research Center funded by the US Department of Energy, Office of Science, Basic Energy Sciences under Award No. DE-SC0016568, and by the Deutsche Forschungsgemeinschaft (DFG) through the Würzburg-Dresden Cluster of Excellence on Complexity and Topology in Quantum Matter–ct.qmat (EXC 2147, Grant No. 390858490). We acknowledge the support of HLD at HZDR, a member of the European Magnetic Field Laboratory (EMFL). A.D.G., W.A.C., and S.W.T. thank J. Wosnitza for financial support and careful review of the manuscript. A.D.G. thanks C. Agosta for crucial help in the data analysis. S.W.T. thanks D. Schiferl for bringing the Parmax and Zylon to his attention.

[1] M. K. Wu, J. R. Ashburn, C. J. Torng, P. H. Hor, R. L. Meng, L. Gao, Z. J. Huang, Y. Q. Wang, and C. W. Chu, Superconductivity at 93 K in a new mixed-phase Y-Ba-Cu-O compound system at ambient pressure, Phys. Rev. Lett. **58**, 908 (1987).

[2] L. Taillefer, Fermi surface reconstruction in high-T_c superconductors, J. Phys.: Condens. Matter **21**, 164212 (2009).

[3] D. LeBoeuf, N. Doiron-Leyraud, J. Levallois, R. Daou, J.-B. Bonnemaison, N. E. Hussey, L. Balicas, B. J. Ramshaw, R. Liang, D. A. Bonn, W. N. Hardy, S. Adachi, C. Proust, and L. Taillefer, Electron pockets in the Fermi surface of hole-doped high-T_c superconductors, Nature (London) **450**, 533 (2007).

[4] D. LeBoeuf, N. Doiron-Leyraud, B. Vignolle, M. Sutherland, B. J. Ramshaw, J. Levallois, R. Daou, F. Laliberté, O. Cyr-Choinière, J. Chang, Y. J. Jo, L. Balicas, R. Liang, D. A. Bonn, W. N. Hardy, C. Proust, and L. Taillefer, Lifshitz critical point in the cuprate superconductor $YBa_2Cu_3O_y$ from high-field Hall effect measurements, Phys. Rev. B **83**, 054506 (2011).

[5] J. Chang, R. Daou, C. Proust, D. LeBoeuf, N. Doiron-Leyraud, F. Laliberté, B. Pingault, B. J. Ramshaw, R. Liang, D. A. Bonn, W. N. Hardy, H. Takagi, A. B. Antunes, I. Sheikin, K. Behnia, and L. Taillefer, Nernst and Seebeck coefficients of the cuprate superconductor $YBa_2Cu_3O_{6.67}$: A study of Fermi surface reconstruction, Phys. Rev. Lett. **104**, 057005 (2010).

[6] T. Wu, H. Mayaffre, S. Kramer, M. Horvatić, C. Berthier, W. N. Hardy, R. Liang, D. A. Bonn, and M.-H. Julien, Magnetic-field-induced charge-stripe order in the high-temperature superconductor $YBa_2Cu_3O_y$, Nature (London) **477**, 191 (2011).

[7] J. Chang, E. Blackburn, A. T. Holmes, N. B. Christensen, J. Larsen, J. Mesot, R. Liang, D. A. Bonn, W. N. Hardy, A. Watenphul, M. v. Zimmermann, E. M. Forgan, and S. M. Hayden, Direct observation of competition between superconductivity and charge density wave order in $YBa_2Cu_3O_{6.67}$, Nat. Phys. **8**, 871 (2012).

[8] S. Gerber, H. Jang, H. Nojiri, S. Matsuzawa, H. Yasumura, D. A. Bonn, R. Liang, W. N. Hardy, Z. Islam, A. Mehta, S. Song, M. Sikorski, D. Stefanescu, Y. Feng, S. A. Kivelson, T. P. Devereaux, Z.-X. Shen, C.-C. Kao, W.-S. Lee, D. Zhu, and J.-S. Lee, Three-dimensional charge density wave order in $YBa_2Cu_3O_{6.67}$ at high magnetic fields, Science **350**, 949 (2015).

[9] F. Laliberté, M. Frachet, S. Benhabib, B. Borgnic, T. Loew, J. Porras, M. Le Tacon, B. Keimer, S. Wiedmann, C. Proust, and D. LeBoeuf, High field charge order across the phase diagram of $YBa_2Cu_3O_y$, npj Quant. Mater. **3**, 11 (2018).

[10] T. Wu, H. Mayaffre, S. Krämer, M. Horvatić, C. Berthier, P. L. Kuhns, A. P. Reyes, R. Liang, W. N. Hardy, D. A. Bonn, and M.-H. Julien, Emergence of charge order from the vortex state of a high-temperature superconductor, Nat. Commun. **4**, 2113 (2013).

[11] H.-H. Kim, S. M. Souliou, M. E. Barber, E. Lefrançois, M. Minola, M. Tortora, R. Heid, N. Nandi, R. A. Borzi, G. Garbarino, A. Bosak, J. Porras, T. Loew, M. König, P. J. W. Moll, A. P. Mackenzie, B. Keimer, C. W. Hicks, and M. Le Tacon, Uniaxial pressure control of competing orders in a high-temperature superconductor, Science **362**, 1040 (2018).

[12] N. Doiron-Leyraud, C. Proust, D. LeBoeuf, J. Levallois, J.-B. Bonnemaison, R. Liang, D. A. Bonn, W. N. Hardy, and L. Taillefer, Quantum oscillations and the Fermi surface in an

underdoped high-T_c superconductor, Nature (London) **447**, 565 (2007).

[13] N. E. Hussey, M. Abdel-Jawad, A. Carrington, A. P. Mackenzie, and L. Balicas, A coherent three-dimensional Fermi surface in a high-transition-temperature superconductor, Nature (London) **425**, 814 (2003).

[14] B. Vignolle, A. Carrington, R. A. Cooper, M. M. J. French, A. P. Mackenzie, C. Jaudet, D. Vignolles, C. Proust, and N. E. Hussey, Quantum oscillations in an overdoped high-T_c superconductor, Nature (London) **455**, 952 (2008).

[15] N. Barišić, M. K. Chan, Y. Li, G. Yu, X. Zhao, M. Dressel, A. Smontara, and M. Greven, Universal sheet resistance and revised phase diagram of the cuprate high-temperature superconductors, Proc. Natl. Acad. Sci. USA **110**, 12235 (2013).

[16] T. Helm, M. V. Kartsovnik, M. Bartkowiak, N. Bittner, M. Lambacher, A. Erb, J. Wosnitza, and R. Gross, Evolution of the Fermi surface of the electron-doped high-temperature superconductor $Nd_{2-x}Ce_xCuO_4$ revealed by Shubnikov–de Haas, Phys. Rev. Lett. **103**, 157002 (2009).

[17] G. Grissonnanche, O. Cyr-Choinière, F. Laliberté, S. René de Cotret, A. Juneau-Fecteau, S. Dufour-Beauséjour, M. È. Delage, D. LeBoeuf, J. Chang, B. J. Ramshaw, D. A. Bonn, W. N. Hardy, R. Liang, S. Adachi, N. E. Hussey, B. Vignolle, C. Proust, M. Sutherland, S. Krämer, J. H. Park, D. Graf, N. Doiron-Leyraud, and L. Taillefer, Direct measurement of the upper critical field in cuprate superconductors, Nat. Commun. **5**, 3280 (2014).

[18] J. L. Tallon, C. Bernhard, G. V. M. Williams, and J. W. Loram, Zn-induced T_c reduction in high-T_c superconductors: Scattering in the presence of a pseudogap, Phys. Rev. Lett. **79**, 5294 (1997).

[19] P. L. Alireza, G. H. Zhang, W. Guo, J. Porras, T. Loew, Y.-T. Hsu, G. G. Lonzarich, M. Le Tacon, B. Keimer, and S. E. Sebastian, Accessing the entire overdoped regime in pristine $YBa_2Cu_3O_{6+x}$ by application of pressure, Phys. Rev. B **95**, 100505(R) (2017).

[20] S. Sadewasser, Y. Wang, J. S. Schilling, H. Zheng, A. P. Paulikas, and B. W. Veal, Pressure-dependent oxygen ordering in strongly underdoped $YBa_2Cu_3O_{7-y}$, Phys. Rev. B **56**, 14168 (1997).

[21] S. W. Tozer, A. W. Kleinsasser, T. Penney, D. Kaiser, and F. Holtzberg, Measurement of anisotropic resistivity and Hall constant for single-crystal $YBa_2Cu_3O_{7-x}$, Phys. Rev. Lett. **59**, 1768 (1987).

[22] S. W. Tozer, J. L. Koston, and E. M. McCarron, III, Variation of the *ab*-plane normal-state resistance and the superconducting transition temperature of a $YBa_2Cu_3O_{7-\delta}$ single crystal to pressures of 13 GPa, Phys. Rev. B **47**, 8089 (1993).

[23] D. E. Graf, R. L. Stillwell, K. M. Purcell, and S. W. Tozer, Nonmetallic gasket and miniature plastic turnbuckle diamond anvil cell for pulsed magnetic field studies at cryogenic temperatures, High Press. Res. **31**, 533 (2011).

[24] See Supplemental Material at http://link.aps.org/supplemental/10.1103/PhysRevB.110.144508 for more details on the TDO technique, high pressure techniques and calibration, additional data and an alternative analysis of the QOs.

[25] A. Savitzky and M. J. E. Golay, Smoothing and differentiation of data by simplified least squares procedures, Anal. Chem. **36**, 1627 (1964).

[26] D. Schoenberg, *Magnetic Oscillations in Metals* (Cambridge University Press, Cambridge, 2009).

[27] N. Tateiwa and Y. Haga, Evaluations of pressure-transmitting media for cryogenic experiments with diamond anvil cell, Rev. Sci. Instrum. **80**, 123901 (2009).

[28] S. Sadewasser, J. S. Schilling, A. P. Paulikas, and B. W. Veal, Pressure dependence of T_c to 17 GPa with and without relaxation effects in superconducting $YBa_2Cu_3O_x$, Phys. Rev. B **61**, 741 (2000).

[29] O. Cyr-Choinière, D. LeBoeuf, S. Badoux, S. Dufour-Beauséjour, D. A. Bonn, W. N. Hardy, R. Liang, D. Graf, N. Doiron-Leyraud, and L. Taillefer, Sensitivity of T_c to pressure and magnetic field in the cuprate superconductor $YBa_2Cu_3O_y$: Evidence of charge-order suppression by pressure, Phys. Rev. B **98**, 064513 (2018).

[30] M. Jurkutat, C. Kattinger, S. Tsankov, R. Reznicek, A. Erb, and J. Haase, How pressure enhances the critical temperature of superconductivity in $YBa_2Cu_3O_{6+y}$, Proc. Natl. Acad. Sci. USA **120**, e2215458120 (2023).

[31] S. Kawasaki, Z. Li, M. Kitahashi, C. T. Lin, P. L. Kuhns, A. P. Reyes, and G.-Q. Zheng, Charge-density-wave order takes over antiferromagnetism in $Bi_2Sr_{2-x}La_xCuO_6$ superconductors, Nat. Commun. **8**, 1267 (2017).

[32] J. S. Olsen, S. Steenstrup, L. Gerward, and B. Sundqvist, High pressure studies up to 50 GPa of Bi-based high-T_c superconductors, Phys. Scr. **44**, 211 (1991).

[33] H. A. Ludwig, W. H. Fietz, and H. Wühl, Calculation of the structural parameters of $YBa_2Cu_3O_{7-\delta}$ and $YBa_2Cu_4O_8$ under pressure, Physica C **197**, 113 (1992).

[34] B. J. Ramshaw, S. E. Sebastian, R. D. McDonald, J. Day, B. S. Tan, Z. Zhu, J. B. Betts, R. Liang, D. A. Bonn, W. N. Hardy, and N. Harrison, Quasiparticle mass enhancement approaching optimal doping in a high-T_c superconductor, Science **348**, 317 (2015).

[35] M. Abdel-Jawad, M. P. Kennett, L. Balicas, A. Carrington, A. P. Mackenzie, R. H. McKenzie, and N. E. Hussey, Anisotropic scattering and anomalous normal-state transport in a high-temperature superconductor, Nat. Phys. **2**, 821 (2006).

[36] A. Damascelli, D. H. Lu, and Z.-X. Shen, From mott insulator to overdoped superconductor: evolution of the electronic structure of cuprates studied by ARPES, J. Electron Spectrosc. Relat. Phenom. **117–118**, 165 (2001).

[37] M. Platé, J. D. F. Mottershead, I. S. Elfimov, D. C. Peets, R. Liang, D. A. Bonn, W. N. Hardy, S. Chiuzbaian, M. Falub, M. Shi, L. Patthey, and A. Damascelli, Fermi surface and quasiparticle excitations of overdoped $Tl_2Ba_2CuO_{6+\delta}$, Phys. Rev. Lett. **95**, 077001 (2005).

[38] B. Vignolle, D. Vignolles, D. LeBoeuf, S. Lepault, B. Ramshaw, R. Liang, D. A. Bonn, W. N. Hardy, N. Doiron-Leyraud, A. Carrington, N. E. Hussey, L. Taillefer, and C. Proust, Quantum oscillations and the Fermi surface of high-temperature cuprate superconductors, C. R. Phys. **12**, 446 (2011).